2

Understanding Mars and Its Atmosphere

RICHARD W. ZUREK

2.1 IN THE BEGINNING

To millennia of naked-eye observers, Mars was just another of the "wanderers" in the night sky, varying in brightness as the months passed and distinguished by its reddish color. The development of good telescopes changed that.

By the late 18th century William Herschel (1784) could confidently say that Mars had an atmosphere. His observation that the recently discovered polar caps on Mars (Cassini, 1666) changed size with season, and the edges of the observed disk were not sharp, pointed to the existence of an atmosphere. That Mars had seasons was evident in Herschel's measurement of the axial tilt of Mars, which was remarkably similar to Earth's. The rotation rate of the planet was also very similar, having been well established by tracking Syrtis Major (Cassini, 1666), one of the darkest features on Mars and the first to have been confidently observed (C. Huygens was the first to draw it, in 1659). Early on, the dark areas were assumed to be seas and their names until recent times (e.g. Mare Cimmerium) reflected that early assumption.

Later observations of hazes (obscurations) and distinct clouds confirmed the atmosphere's presence, although the planet's low albedo suggested that there was less air than on Earth. With the advent of much improved photographic capabilities early in the 20th century, Mars was seen to be larger and fuzzier in blue filters than in red, and it was possible to distinguish reliably "white" clouds from "yellow" ones (e.g. Slipher, 1962; Martin et al., 1992). And yet clouds were sufficiently rare that their presence was worthy of note by observers. Viewing the planet's surface was difficult, not just due to the often great distance between Earth and Mars, but also because the Earth-based observer was looking up through Earth's atmosphere and down through that of Mars. Even so, a fascinating vision of our planetary neighbor was taking shape.

By the early 20th century, particularly in the perspective popularized by Percival Lowell (Lowell, 1895, 1896, 1906, 1908), Mars was an older Earth, its mountains worn down and much of its water lost to space or frozen in its crust (a dichotomy we investigate even today). The spidery network of canals drawn by Lowell appeared artificial and he took it as evidence of a race of intelligent beings struggling against a changing climate. Through global engineering, the Martians in his view were redistributing the precious remnant of the planet's water that melted seasonally at the poles to irrigate what otherwise was a desert planet. No mountains had been reported to bar their path. The atmosphere was there, but like the major deserts of the Earth, rain was rare, with most condensation coming as snow near the poles. Each spring, a wave of darkening (see Lowell, 1906) was reported to sweep down from the poles; this was the water coursing through the channels and canals towards the equator, nourishing and darkening what were then regarded as vast regions of vegetation. Except for the larger scale, this was not unlike the irrigated desert in the American southwest where Lowell had built his observatory to view Mars.

It was suspected that Mars, being a smaller planet, would have a less dense atmosphere than Earth. This thinner atmosphere, together with the planet's greater distance from the Sun, meant that the ground and atmosphere would be colder, but in the Lowellian view, it was warm enough. However, the liquid that remained would have to be carefully husbanded. It all made a kind of sense to the general public, for whom the idea of life on other planets seemed no more radical than Darwin's recent theory of evolution.

Scientifically, Lowell and his ideas were very controversial even in his own time. In a scathing review of Lowell's work, Alfred Russel Wallace (1907), famous as an independent developer of the theory of evolution, declared that Mars would be much too cold and that Mars was "not only uninhabited by intelligent beings … but is absolutely UNINHABITABLE". The canals themselves were much debated. Many observers, particularly in the cadre of professional astronomers, simply did not see them. Even many of those who did (and there had been reports even before Schiaparelli's report on the 1877 opposition had brought them into wider view) saw them as disjointed or irregular – few saw the numerous fine lineae and geometric pattern that argued for their artificiality.

Today we know that the canals, especially those quasi-linear versions pointing to artificial origin, have no physical correspondence on the planet; they were the results of the great difficulty of peering through two shimmering atmospheres trying to see features that would have been at the very limit of detectability even had they existed. However, the existence and nature of the canals and of the dark areas were debated well into the 1960s, long after Lowell's death in 1916 and into the early days of the space age. The "wave of darkening" also seemed to be different things to different observers (see the discussion in Martin et al., 1992). Today we know that it is the wind and its redistribution of bright dust that affects the surface albedo. This can darken vast regions, sometimes the cumulative action of hundreds of dust devils leaving their mark. And the belief that there were no mountains on Mars was just wrong, as Mars has major topography, comparable to the continental highs and oceanic basin lows on the Earth. Its Olympus Mons is the tallest of the known

volcanoes in the Solar System, reaching ~16 miles above the surrounding plains. But this was not known until Mariner 9, the first Earth spacecraft to orbit another planet, observed the summits of four major volcanoes towering above a global dust haze in 1971.

To convince his critics, Lowell worked – as a good scientist should – to acquire more data that would support his theories. He sought experts who could apply then state-of-the-art spectroscopic instruments in an attempt to quantify how much water was in the Mars atmosphere. Water vapor absorbs sunlight in specific spectral bands. The difficulty is to separate the absorption of sunlight that is reflected from Mars from that absorbed in the more massive – and wetter – atmosphere of the Earth. Lowell and his co-workers realized that the relative motions of Earth and Mars would Doppler-shift the Mars spectral lines away from the Earth lines. Thus, the time to try to detect water in the Mars atmosphere was not when the planets were closest, lined up with the Sun during opposition, but when they were almost in quadrature. The planets were farther apart then, but the greater relative motion could separate the absorption features of the two planetary atmospheres. This approach is used today in our ground-based search for trace gases such as methane in planetary atmospheres. Unfortunately for Lowell, his measurement attempts were at best inconclusive. Ironically, it would be improved spectroscopic methods that first provided solid evidence that Mars and its atmosphere today were not as Earth-like as they once had seemed.

2.2 1962–1972: A DECADE OF CHANGE WITH THE FIRST WAVE OF SPACECRAFT EXPLORATION

In the mid-1950s, de Vaucouleurs (1954) summarized the estimates at that time of atmospheric pressure on Mars. Based on indirect measurements, such as the polarization of reflected sunlight, the Mars surface pressure was estimated at 85 hPa (mbar), as compared to the Earth's average surface pressure of approximately 1 bar (1000 hPa). This was lower than had been expected by many earlier scientists, but not greatly so. In a remarkable book, the *Exploration of Mars* published in 1956, Werner Von Braun and Willy Ley summarized the current knowledge of Mars and outlined how one might explore the planet with emerging rocketry (Von Braun and Ley, 1956). Their Mars landing craft had extensive wings – not unlike the recent space shuttle – because they were still expecting atmospheric pressures on Mars to be ~10% that of Earth – not the ~1% that we know today.

In 1947 Kuiper analyzed bands of CO_2, recorded in telescopic spectroscopic data, to derive an amount of CO_2 for Mars that was only twice that in the Earth's atmosphere (Kuiper, 1952). Because the absorption bands observed could be pressure-broadened, the amount of derived CO_2 was inversely proportional to the square root of the total ambient pressure, which could include hard-to-detect gases like nitrogen or argon. In the 1960s, Spinrad et al. (1963) did what Lowell had failed to do: detect water vapor in the Mars atmosphere. And Kaplan et al. (1964) derived a CO_2 abundance from a weaker CO_2 absorption band observed by Spinrad et al. (1963) that was nearly pressure-independent. When combined with Kuiper's measurements, Spinrad et al. (1966) derived a total surface pressure of 25±15 hPa and 14±7 pr μm for water vapor (1 pr μm is the equivalent depth of water if all the water vapor in a column were condensed to liquid; a typical value for the Earth's column vapor – excluding liquid water drops – is ~5 pr cm, an amount ~3500 times greater than the Spinrad et al. value for Mars). These landmark results indicated a much thinner atmosphere than had been previously suspected (Owen, 1992). This result was soon to be tested in a very novel way.

The clincher came when the first spacecraft flew by Mars in 1965. During its encounter, Mariner 4 transmitted a radio signal through the Mars atmosphere as the spacecraft disappeared behind the planet as seen from Earth (a radio occultation event). Analysis of the refraction of that radio signal by the atmosphere indicated that the total atmospheric pressure was 4–6 hPa. Not only was the atmosphere thin, it would have to be composed almost entirely (>90%) of carbon dioxide. This newly measured pressure could be significantly below the triple point for water (6.1 hPa), so liquid water was not to be expected on the Martian surface. This seemed consistent with impressions left by the Mariner 4 photographs of a narrow swath of the Martian surface that showed only a heavily cratered, Moon-like surface.

A straightforward one-dimensional (vertical) energy balance calculation by Leighton and Murray (1966) showed that a cold Mars atmosphere composed of CO_2 would have another very un-Earth-like feature: temperatures in the winter polar region would be so cold (~140 K) that CO_2, the major constituent of the atmosphere, would condense out – a lot of CO_2. This implied that the seasonal snow was CO_2 (not water) and the polar caps themselves might well be composed of dry (CO_2) ice, not water ice. Furthermore, the mass of the atmosphere would vary throughout the Mars year, with two maxima and two minima, as the atmospheric mass cycled between the two polar regions in response to the seasonally changing insolation.

By the late 1960s, Sagan and Pollack (1969) concluded that albedo changes – even the seasonal "wave of darkening", which seemed such a robust indicator of vegetation – were more likely due to the emplacement and removal of bright, fine-grained dust. (Scattering of sunlight not solely by gas, but also by dust suspended in the atmosphere would have led to the earlier overestimation of the atmospheric pressure derived indirectly from radiometric and polarization measurements.) The seasonal timing of the dust removal was attributed to the seasonal migration of storms from high to low latitudes, as on Earth. This might be aided by the inferred Martian outflow from the poles, a "sublimation" flow in the spring (reversed as a "condensation" flow in the fall) of a significant fraction of the total CO_2 inventory subliming from (condensing onto) the polar caps.

Images from the Mariner 4, 6, and 7 flybys of Mars had all largely sampled its southern hemisphere, revealing it to be heavily cratered. No canal-like features were seen. This, along with the atmospheric results and the demonstration that the seasonal surface albedo changes were meteorological rather than biological in nature, spelled the end of the Lowellian view

of modern Mars as an older Earth-like planet. Interest in this Moon-like Mars plunged, but fortunately development of the next Mars mission was already underway. In the meantime, the meteorologists were making progress.

Seymour Hess (1950) published the first "climatology" of the Mars atmosphere. This paper was the first ever published in the *Journal of Meteorology* (now the *Journal of the Atmospheric Sciences*) that dealt with the atmosphere of another planet. The climatology was based on surface temperature measurements by Coblentz and Lampland (1927) and a mere 18 wind vectors derived from tracking clouds. Obviously, Hess relied on his experience as a terrestrial meteorologist and the theoretical relationships between temperature and winds that had been developed already for weather forecasting on Earth. (Hess would later lead the Viking mission meteorology team.)

Observations in the 1960s indicating that the atmosphere had low mass, was mainly composed of carbon dioxide, and rested on a desert-like surface with little heat capacity, had other implications for understanding the Mars atmosphere. In a series of papers (Goody and Belton, 1967; Gierasch and Goody, 1967, 1968), results from one-dimensional radiative–convective transfer calculations indicated that such a Mars atmosphere should respond quickly to solar and infrared radiation. In an atmosphere with so little water vapor, latent heating would be small, unlike the Earth, so heat transport and exchange would be dominated by radiation and dry convection above a heated surface. Given the near absence of clouds and lacking large amounts of trace gases like ozone and water vapor, the Mars atmosphere would let sunlight pass through nearly unattenuated and it would be absorbed by the surface. With little ability to store the heat (again partly a consequence of no liquid water), the surface would undergo a large daily temperature variation.

The atmosphere would be heated by convective and sensible heat transfer from the surface and by some absorption by CO_2 of the infrared radiation emitted from the surface. Although CO_2 is a potent greenhouse gas, there is not much of it in the thin Mars atmosphere, and so air temperatures would rapidly decrease with height through a planetary boundary layer (a few kilometers deep during the day, perhaps several hundred meters at night) and then stay relatively constant until high in the atmosphere (above ~90 km), where temperatures would increase again due to absorption of ultraviolet solar radiation. Our current, more detailed understanding of radiation in the Mars atmosphere, the factors that control it, and how we compute the resulting forcing for numerical models, is discussed in Chapter 6).

This control of temperature in a radiative–convective environment can be expressed in terms of the exponential folding time it would take for an atmospheric temperature perturbation to dissipate by radiation back to a purely radiatively determined equilibrium. On Earth, this time is several days; on Mars, it is a day or so. That meant that it would be more difficult to transport heat, for example, into the polar regions to restrict CO_2 condensation, and that diurnal variations on Mars should be larger in amplitude than even above the highest deserts of the Earth. To understand this quantitatively, it was necessary to put all this new information together in a four-dimensional simulation of the Mars atmospheric state and circulation. Fortunately, such an experiment was already underway.

Yale Mintz (1961) had predicted, based upon terrestrial experience and meteorological scaling arguments, that Mars should have winter storm systems like those on Earth (i.e. baroclinic systems). In the summertime, however, a single Hadley-like cell would dominate, with a physical overturning of the atmosphere in which preferentially heated air rising above the more strongly heated low latitudes moves poleward, cools radiatively, and sinks in mid-latitudes while adiabatically warming. The rising and sinking branches of these cross-equatorial circulations would alternate hemispheres with the seasons.

Leovy and Mintz (1969) tested these ideas by adapting a then state-of-the-art Earth general circulation model that had been developed at UCLA. Given the limitations of their computers (they used the medical school's computer, which was the fastest available to them), the model was restricted to two levels in the vertical, and a horizontal grid with 7°×9° in latitude and longitude (922 points, including the two poles). The model input parameters had to be chosen despite uncertainties in atmospheric composition (it had been suggested that the inert gas argon could compose up to 40% of the atmosphere), almost no knowledge of surface topography (none was assumed in the model), in details of radiative transfer, and in surface heat capacity (Leovy (1966) derived a set of surface thermal inertias). A novel feature for Mars was that the model atmosphere had to gain or lose mass as dictated by the polar radiation budget, unlike the mass conservation typically assumed for Earth.

Their results confirmed Mintz's earlier theoretical expectations to some extent. Storm systems embedded in the polar jet streams were prominent, with their changes over a few days dominating variability at high latitudes. But even these were not vigorous enough that their poleward heat transport would stop condensation in the cold winter polar night. Radiation loss and latent heating of the condensing CO_2 were still the dominant terms in the polar energy balance. Also prominent in the simulations were large diurnal fluctuations in temperature, wind, and pressure. These were large enough to be the second largest component of variation at lower latitudes, behind the seasonal variations but ahead of the day-to-day changes. On Earth, these fluctuations, driven by each day's cycle of solar heating, are muted by the larger thermal mass of the atmosphere and by the action of liquid water, with its large heat capacity, both in the oceans and in the hydrated land. Finally, a Hadley-like circulation did develop in the model simulations, but its structure was more complex (and limited in latitude) than the analytic theory had predicted.

This was a pioneering experiment in many ways. It was the first numerical simulation of the general circulation of another planetary atmosphere, and it used what was nearly the state-of-the-art tools and methodology that were being used for study of the Earth at that time. This approach of adapting advanced four-dimensional circulation models to Mars almost as soon as they were developed for Earth studies continues through the present time (see Chapters 8 and 9). The main difficulties were the limited computing capability and the paucity of data that

could be used to define the boundary conditions, to inform the physical parameterizations, and to validate the results. One of the key omissions of this initial general circulation experiment was the (lack of) heating and cooling by airborne dust.

Observers on Earth historically viewed Mars when it was close at opposition, a period that varied in a synodic 17-year cycle so that different seasons were viewed at different oppositions. Some of these oppositions had better viewing than others because the elliptical orbit of Mars would bring the planet closer to the Sun and Earth when Mars was at its perihelion, which currently occurs towards the end of southern spring on Mars. (This seasonal date varies on timescales of hundreds of thousands of years.) Schiaparelli first gave prominence to the *canali* as a result of observing during the favorable opposition of 1877. In another such opposition in 1956, a major dust event was observed for several days. Such events were regarded as rare, but that perception was about to change.

In 1971 Mariner 9 went into orbit around Mars in the middle of a truly global dust storm that had been raging for more than a month before its arrival and which continued to obscure the surface from its view for several months afterwards. Dust was raised 70 km above the surface, with a thin ice haze detached above it (Anderson and Leovy, 1978), and all of the planet, even the poles, was affected. Middle atmospheric temperatures became much warmer for a time (Hanel et al., 1972).

As the atmosphere cleared, a new Mars was revealed (Hartmann and Raper, 1974) due to the global coverage, higher resolution, and better signal-to-noise ratio of the Mariner 9 cameras. A handful of dark spots visible early above the dust pall were revealed to be the summit calderas of massive volcanoes; channels – not canals, but massive channels – were etched on the planet's surface, with converging valley networks revealed in scattered locales. The polar caps and surrounding terrains were extensively layered, suggesting episodic deposition in a series of ice ages, perhaps triggered by the effects of changes in orbital eccentricity and rotation pole obliquity (Chapter 16). Also revealed was a planetary dichotomy, with heavily cratered highlands in the southern hemisphere (which had been overflown by the earlier Mariner spacecraft) and vast, smooth, low-lying plains in the northern hemisphere.

Now interest in Mars soared, as this was once again a dynamic world, one that may have been more Earth-like in its past, one whose climate had obviously changed, and one perhaps capable of change even today. That global dust storm – which remains the most extensive yet seen on Mars – in particular had a definitive impact on thinking about Earth's climate. It was now a plausible reality that the sky could be darkened over most of the Earth for months by a dust cloud from an asteroid impact or even by dust and smoke from a nuclear conflagration. Mars had caught our attention.

For the atmospheric scientists, whose interest in Mars had not waned, there were two new major features that needed to be taken into account: the role of dust in heating the atmosphere (Gierasch and Goody, 1972); and the effect of the large planetary-scale topography. Both affect the basic temperature structure and the general circulation of the Mars atmosphere.

2.3 VIKING: THE SECOND WAVE OF SPACECRAFT EXPLORATION OF MARS

The highly ambitious Viking mission – two orbiters deploying two landers to the surface of Mars – was focused on the search for life. It was predicated on an assumption that, if life had developed anywhere on the planet, it would be everywhere and could be detected by analysis of any soil sample. The orbiter instruments – multispectral cameras, a thermal infrared radiometer, and a water vapor mapping spectrometer – were flown in the hopes that they could help with site selection in terms of safety (surface properties) and of life detection potential (water sources and/or "hot spots"). Launched in 1975, the orbiters and landers explored Mars from 1976 until contact with the last spacecraft (Viking Lander 1) was lost in November 1982. While it did not detect life, Viking expanded our knowledge of Mars immensely, particularly in terms of surface properties and climate.

Isotopic measurements made during entry of the Viking Landers indicated a loss of the lighter isotopes of nitrogen; this argued for massive loss of an early Mars atmosphere through escape to space. Atmospheric measurements from orbit and by the landed meteorology packages were conducted for more than one Mars year. These gave a much better idea of the annual climatology and its inter-annual variation (Hess et al., 1977). In particular, the annual cycles of atmospheric water vapor revealed a seasonal progression of water to low latitudes from a permanent water ice cap at the north pole, eerily reminiscent of past arguments (but no darkening vegetation!) (Farmer et al., 1977).

Measurements in parts of three Mars years also revealed multiple episodes of very large dust storms during the southern spring and summer, the perihelic seasons when Mars is closest to the Sun (Chapters 3 and 10) and insolation is most intense. The effects of dust heating amplifying the already large daily fluctuations of temperature, pressure, and wind and the role of topography in modulating these variations were prominent and soon the subject of numerical simulations (Chapters 6 and 9). Atmospheric dust was now prescribed in models, and there were two sites of meteorological data against which to compare. The richness of these meteorological fields is exhibited by looking at the surface pressure records recorded by the Viking Landers at just two places on Mars (Figure 2.1).

The first thing in Figure 2.1 that catches one's attention is that ~25% of the Mars atmosphere disappears and reappears twice in a Mars year. This is due to the condensation/sublimation of the CO_2 atmosphere onto the polar caps in fall/spring, noted earlier. The differences in the twice-yearly maxima and minima reflect the very elliptical orbit of Mars, with a longer and cool aphelic northern spring–summer, and a shorter and warm perihelic southern spring–summer. The offset of the two curves reflects the ~1.5 km difference in their elevations. Third, there are different meteorological regimes evident at the two Viking Lander sites, with VL1 at 22.4°N (corresponding latitude on Earth is Hawaii) and VL2 at 48°N (on Earth, close to the U.S.–Canada boundary). The quasi-regular variation on timescales of a few days is apparent at the higher latitude in winter–spring and reflects the baroclinic storm systems that feed on the potential energy inherent in the large

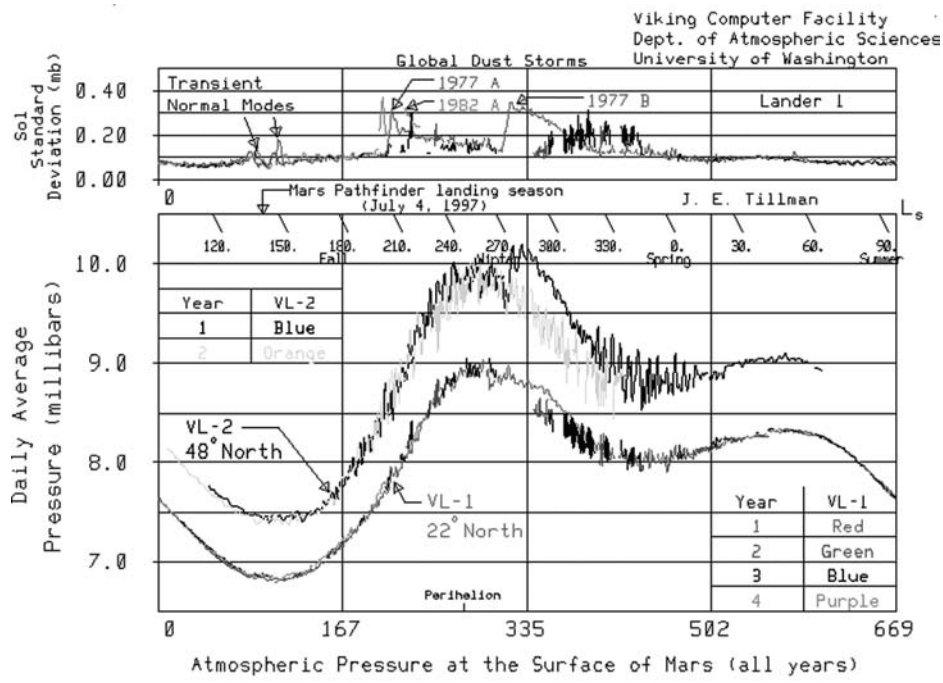

Figure 2.1. The Viking Lander pressure curves measured on the surface at 23°N and 48°N by the Viking Lander 1 and 2 meteorological sensors, respectively. The daily (sol) average and the sol standard deviations are shown. The bottom axis is given in sols, dated from the arrival of Viking Lander 1; the upper axis of the lower panel gives the time of year in L_s, the areocentric longitude of the Sun. The effects of topography, latitude, weather, and even a nearly global dust event are shown (see text). Figure provided courtesy of James Tillman, a veteran of the Viking mission and Viking Lander Meteorology Team. A black and white version of this figure will appear in some formats. For the color version, please refer to the plate section.

latitudinal temperature gradients that develop in those seasons (Chapter 9). Variation at the lower-latitude site is driven by the annual migration of the subsolar point and its associated heating. This drives the rising branch of the overturning circulation and its cross-equatorial transport.

Daily fluctuations of the meteorological fields are shown as the standard deviation of surface pressure within a Martian day in the top panel of Figure 2.1. Note the large amplification of these fluctuations during the major dust storms. These are the thermal atmospheric tides, so-called in analogy to variations of the sea surface on Earth due to the gravity of the Moon and Sun. On both Earth and Mars the atmosphere also responds to these gravitational perturbations by the Sun and moons, but the resulting variations are small compared to the global oscillations driven by the daily heating of the atmosphere. On Earth, this heating is due to ozone and water vapor absorption of sunlight and by convective heating (Chapman and Lindzen, 1970); on Mars, it is due to absorption of sunlight by CO_2 and airborne dust and convective heat exchange with the surface (Lindzen, 1970; Zurek, 1976).

In Figure 2.1 there is an increase in daily mean surface pressure at both Viking sites during the first Mars year (dark curve), though more pronounced at the more northern site, at L_s ~ 280°. (L_s is the areocentric longitude of the Sun measured from vernal equinox, so that L_s = 0°, 90°, 180°, and 270° mark the beginning of northern spring, summer, fall, and winter, respectively; a Mars year is 687 days or 670 sols long (Table 2.1; a sol being a Martian solar day of 24^h37^m).) This increase in surface pressure is due to the second of two planetary-scale dust storms that occurred during the first year of Viking observations. Occurring near the southern summer solstice, when Mars is near perihelion, this dust storm drove a massive overturning of the atmosphere, with air rising in the dustier atmosphere and higher insolation of the southern subtropics. The air crossed the equator and sank in the northern subtropics and middle latitudes, producing a zone of downwelling convergence increasing the column air mass and thus the surface pressure. The greater the heating, the more vertically extended the circulation cell and the further poleward this descending branch can go. On Earth this zone is in the subtropics and low mid-latitudes and accounts for the latitudinal zones of the major deserts on the planet. On Mars this zone can move further poleward as the dust haze that heats the atmosphere increases in opacity, altering the vertical extent of the associated solar heating by dust absorption. Given the transience of dust events on Mars, this expansion of the zone of high surface pressure is temporary on Mars, moving so far north only in those years with major dust events.

After Viking there was a hiatus in the exploration of Mars by spacecraft. While highly successful in expanding our knowledge of Mars, the expense of the mission and the disappointment of not detecting evidence of life, past or present, gave pause to further exploration.

But that did not halt progress. The long-lived Viking mission had left a gold mine of data that would take many years to digest. Furthermore, improved Earth-based observations – both

Table 2.1. *Fundamental metrics for Mars and Earth.*

Metric	Mars	Earth	Ratio
Radius (equatorial) (km)	3396	6378	0.53
Area (10^6 km^2)	144.8	510.1	0.28[a]
Solar day (Mars sol, Earth day, h)	24.66	24.00	1.027
Sidereal day (h)	24.62	23.93	1.029
Rotation frequency, Ω (sidereal, 10^{-5} s^{-1})	7.088	7.292	0.972
Year[c] (Mars sols)	668.6,	355.6,	1.88
Year[c] (Earth days)	687.0	365.25	
Orbital semi-major axis[b] (AU)	1.524	1.000	1.52
Orbit eccentricity[b]	0.0935	0.0167	5.60
Perihelion[b] (AU)	1.38	0.98	1.41
Aphelion[b] (AU)	1.67	1.02	1.64
Obliquity (tilt of rotation axis)[b] (deg)	25.19	23.44	1.075
Gravity (surface, m s^{-2})	3.71	9.80	0.38

[a] This is nearly the same as the land area of the Earth (29%).
[b] These orbital parameters vary much more for Mars than they do for Earth.
[c] By convention, Mars years start with the northern spring equinox when the areocentric solar longitude $L_s = 0° = 360°$. Many scientists analyzing modern spacecraft data follow the Clancy et al. (2000) convention that counts the Mars year of the 1956 great dust storm as Mars Year 1. In this convention, Mars Year 33 started June 18, 2015.

ground-based high-resolution spectrometers and orbital observatories like the Hubble Space Telescope – were still observing Mars (Chapter 3). Their purpose was largely to detect trace gases and to characterize inter-annual variability in dust storm events and in basic temperature structure. In parallel, ever more sophisticated tools were being developed to simulate the observed atmospheric phenomena. Atmospheric general circulation models (GCMs) were now prescribing dust hazes and planetary-scale topography, and they were being run with increased spatial resolution and vertical range; e.g. simulations were done using a six-layer model just prior to the arrival of the Viking spacecraft. Even so, the vertical domains in the models were inadequate to describe the deep Hadley-type circulations that could develop in a dusty atmosphere or the atmospheric tides, with their vertically propagating components. Quasi-analytic models, such as zonally symmetric (two-dimensional in latitude and altitude) (Haberle et al., 1982), and linear atmospheric tidal models (Fourier components in time and longitude), were still used to provide some insight.

For the atmospheric tidal theory, these models indicated that daily changes in meteorological fields were not functions purely of local time, with minima and maxima following the Sun's apparent westward motion. In particular there was a class of eastward-propagating components (Kelvin modes) that could be efficiently excited (as in resonance) by longitudinal variations in topography and column dust opacity (Zurek, 1976). The presence of such a tidal variation was confirmed via temperature observations by Mariner 9 (Conrath, 1976) and Viking surface pressure data (Zurek and Leovy, 1981). Thus, the structure and temporal variation of these daily fluctuations were more complex than had been first anticipated. Interestingly, the observed prominence of the twice-daily tide during very dusty periods on Mars could be demonstrated to be the same effect as for the Earth's semidiurnal pressure tide being larger than its diurnal counterpart, despite the latter being the bigger component of the daily insolation variation. On both planets, it was heating at higher elevations (in a dust haze on Mars and by stratospheric ozone on Earth) adding up to make the local tide with the larger vertical wavelength (i.e. the semidiurnal tide) the dominant component of surface pressure variation (Chapman and Lindzen, 1970; Zurek, 1980).

Work with these models in the post-Viking period helped illuminate many observations made during the Viking missions. A long hiatus in missions to Mars followed, but there was an effort through various data analysis programs and workshops to exploit the datasets that had been gathered and to utilize increasingly sophisticated models to understand the resulting clues about the present and past climates of Mars. As the prospects for a new (third) wave of Mars exploration loomed on the horizon, the knowledge gained from these efforts was summarized in a massive book (appropriately called *Mars*) covering all the many aspects of Mars, including 420 pages spanning several chapters on the atmosphere of Mars alone. Here are some summary highlights (Kieffer et al., 1992, and references therein):

- The mostly carbon dioxide atmosphere held trace amounts of water vapor and ozone, anticorrelated in their seasonal and spatial distributions by photochemistry, while isotopic signatures of trace nitrogen pointed to massive loss over time of atmospheric gases via escape to space processes.
- The existence of vast channels and valley networks, apparently carved by water, indicated massive water activity on early Mars (3.5–4 Ga).
- The puzzling nature of the polar caps: the low-lying, but still mile-thick, north polar cap, with its layers of water ice exposed during summer, but nearly crater-free surface; the high-altitude, apparently older south polar cap, with a thin layer of carbon dioxide ice persisting throughout the hot southern summer, with the survival of that ice dependent on a remarkably high surface albedo, which appeared to brighten as the seasonal insolation increases.
- Large-scale topography from surface pressure and radio occultation data had outlined the hemispheric dichotomy (heavily cratered, high-altitude southern hemisphere punctuated by the giant impact basins of Hellas and Argyre versus relatively smooth and featureless northern low-lying plains), the massive volcanoes of Olympus Mons, the Tharsis plateau and Elysium, and the Valles Marineris rift systems, the latter extending across the equivalent width of the continental U.S.
- The basic cycles of dust, water, and carbon dioxide:
  - A basic understanding of the recycling of a major fraction of the largely CO_2 atmosphere, controlled by

radiative energy balance and subsurface heat conduction. However, it was surprisingly difficult for the GCMs to get this right, within the observational constraints of polar surface albedo, etc.
  - The episodic nature of the larger dust storms, occurring in some years but not others, but typically in southern spring and summer, a so-called great dust storm season. Local dust storms had been observed in all seasons, but the statistics of their occurrence and nature were poor due to the non-systematic coverage provided by the Viking Orbiters, which were also tasked to provide communication with the landers.
  - An annual, global cycle of water vapor, with the north polar cap being the major source of atmospheric water for the planet, but with major uncertainties as to the role of the regolith as a source or sink, or the extent to which the cycle was closed.
- Apart from the surface pressure and wind measurements at the two Viking Lander sites, there were few quantitative aspects determined regarding the atmospheric circulation. Basic clues came from observations of atmospheric tracers like ozone, water vapor, and dust and of surface wind streaks. A remarkable warming of the north polar atmosphere during the largest of the 1977 dust storms was observed and attributed to adiabatic warming of the downwelling branch of a Hadley-like circulation extending all the way to high latitudes. However, models continued to be the main means of estimating the general circulation.
- Basically unknown were the magnetic properties of the planet and details of the upper atmosphere. For example, there were less than two dozen profiles of the ionospheric peak in the upper atmosphere, observed by the Mariner 9 Ultraviolet Spectrometer data (Stewart et al., 1972). Using those data, A. I. Stewart estimated a natural variability (one-sigma) of the upper atmosphere from orbit to orbit of ~30% in atmospheric density, a surprisingly robust number confirmed by later aerobraking Mars orbiters operating above ~100 km (Tolson et al., 2007).

A major discovery not captured in *Mars* during this period came from ground-based microwave spectrometers. In observations by Clancy (also see Chapter 5) the Mars atmosphere appeared to be colder and cloudier than Viking had reported, particularly during northern spring and summer, when Mars was near aphelion in its eccentric orbit and the atmosphere was relatively dust-free. Inter-annual differences in the atmosphere during southern spring and summer were easily ascribed to the episodic occurrence of planetary-scale dust storms. These microwave ground-based observations of Mars during its northern spring–summer suggested a major shift in the modern Mars climate. Subsequent observations and further analysis of Viking infrared thermal mapper data showed that the "aphelion cloud belt", a low-latitude zone of thin water ice clouds, had been present during the Viking era too (Tamppari et al., 2000). While not indicative of a major change in climate, Clancy's discovery showed that a new element (ice clouds) had to be taken into account if we were to advance our understanding of atmospheric structure and circulation.

2.4 THE THIRD WAVE OF SPACECRAFT EXPLORATION OF MARS

Nearly continuous remote sensing from orbit of the Mars atmosphere, a need elegantly articulated in *Mars* (Kieffer et al., 1992), has been a signature feature of the modern program of Mars exploration. However, success was not immediate. An ambitious attempt to restart Mars exploration was stymied first by the loss in 1991 of Mars Observer. A shift to smaller, less expensive, spacecraft resulted in major successes with Mars Pathfinder conducting landed operations for two months in 1997 and, with an eight-year highly productive Mars Global Surveyor mission in 1998. However, further cost-cutting as part of a "faster, better, cheaper" strategy ultimately resulted in the loss of both the Mars Climate Orbiter and the Mars Polar Lander, launched in the 1998–1999 opportunity.

A reinvigorated Mars Exploration Program (Chapter 3) was developed following the loss of those two missions and has resulted in major successes for NASA with the launches in 2001 of the Mars Odyssey (ODY) Orbiter, of two Mars Exploration Rovers (MERs) in 2003 (Opportunity and Spirit), of the Mars Reconnaissance Orbiter (MRO) in 2005, the Phoenix Lander in 2007, and the Mars Science Laboratory (Curiosity) Rover in 2011. The European Space Agency (ESA) also launched in 2003 a highly capable orbiter, Mars Express (MEX), which also carried a small probe, Beagle II, which unfortunately was lost during landing. (Twelve years later, a former member of the operations team detected the craft in an MRO high-resolution camera image, which showed that the craft had successfully landed but only partially deployed its solar panels, blocking the radio antenna.)

Launched in 2007, Phoenix landed at high northern latitudes on Mars, where it operated from May to September 2008 before the harsh northern winter ended the mission. (Images taken the following spring show that the weight of accumulated wintertime CO_2 frost had broken the solar panels.) Contact with the Spirit Rover was lost in 2010 after seven years of exploration in Gusev Crater and its Columbia Hills in what was originally a 90 sol mission. The Opportunity Rover continues to operate 13 years later. (The rate of dust accumulation on the Mars Pathfinder solar panels during its short mission suggested that the MER craft would be starved for solar power after 90 sols. Fortunately, winds have periodically removed dust from the MER panels, renewing solar power generation.) Mars Odyssey, Mars Express, and MRO all continue to explore and return data from Mars orbit, with MRO having returned 300 Tbits (as of March 2017) of often-compressed science data, an amount greater than all other deep-space planetary missions.

In September 2014, two new orbiters, NASA's Mars Atmosphere and Volatile Evolution (MAVEN) mission and the India Space Research Organization's (ISRO) Mars Orbiter Mission (MOM), joined the three working orbiters and two operating rovers (Opportunity and Curiosity). MAVEN's focus during its one Earth year prime mission has been the solar wind interaction with the Mars upper atmosphere and the mechanisms by which volatiles can escape from Mars. Its observations will test models of present escape (Chapters 14 and 15), hopefully adding enough detail of current processes to permit extrapolation back into the ancient regime, when the Sun was ultraviolet-bright, but radiated less total energy (see Chapter 17).

Three meteorological stations have been landed since Viking (Chapter 3). Two had limited lifetimes: Mars Pathfinder operated near the equator for two months in 1997, and Phoenix was limited in 2008 to a summer of observations at a high northern latitude. The third (Curiosity) has operated since 2012. In addition to meteorological measurements, these have provided ground truth for the opacity record by upward-looking observations of the extinction of sunlight at the landing sites (Chapter 10). The Mars Exploration Rovers did not carry meteorological sensors given their tight mass constraints and presumed 90 sol lifetimes, but they have provided many years of overhead atmospheric opacity measurements.

This third wave of exploration of Mars by spacecraft has steadily improved the spatial resolution of our global coverage of Mars. We now have global datasets of the surface which have increased the spatial resolution of visual images of Mars from the 200 m or more per pixel of Viking to more than 99% of the planet covered in a panchromatic band at 6 m/pixel, stereo color images for more than half the planet at resolutions of ~20 m/pixel, and a carefully selected 2.5% of the planet at an unprecedented 30 cm/pixel, a fifth of which is in color. Highly magnetized remnants of the crust, but only in the oldest terrains, have been mapped, indicating that Mars once had a global magnetic field that disappeared early in the planet's history (~4 Ga; Acuna et al., 1999)[1]. The radical reduction in that global field strength possibly led to a much more accelerated loss of atmospheric mass due to the actions of the solar wind, as it could now sweep through the upper atmosphere (Chapters 15 and 17). Characterizing escape processes is the ongoing goal of the MAVEN mission.

Mars topography is now known from laser altimetry to a precision of ~3 m averaged in 1 m spots approximately 100 m apart along the ground track (see Smith et al., 1999). Due to the spacing between ground tracks, this yields a *global* topography with resolutions of ~1 km in latitude and 2 km in longitude at the equator (Smith et al., 2001). Valley networks can be shown to have had streams running downhill and inverted streambeds speak to extensive erosion on Mars some time in its history. The thermal inertia and albedo of the surface are now characterized at 100 m/pixel (Fergason et al., 2006) permitting, amongst other things, calculations of the ice holding capacity of the near surface.

The actual distribution of near-surface ice (at <1 m depth) has been determined using the orbital observations of subsurface/surface hydrogen in footprints a few hundred meters across (Boynton et al., 2002; Feldman et al., 2002; Mitrofanov et al., 2002). These data show very shallow ice in the middle to high latitudes and adsorbed water and/or hydrated minerals in many locations at lower latitudes. The presence and depth of ice (a few centimeters of overburden at 68°N on the northern plains) was confirmed by the Phoenix Lander digging locally into the Martian ground (Smith et al., 2009; Mellon et al., 2009).

As noted earlier, a signature achievement of the recent exploration program has been acquisition of a multi-year record of atmospheric fields. Daily, global weather maps at ~1 km resolution, together with seasonal maps of column dust opacity and zonally averaged water vapor, now span a Mars decade and reveal a wealth of phenomena: dust storms, weather systems, jet streams (Chapters 5, 9, and 10). Systematic maps of column ozone and carbon monoxide have been added to that record since 2006 (Chapter 13). A greatly expanded database of Mars clouds, including multiple new cloud types such as CO_2 hazes high in the middle atmosphere, together with refined estimates of their particle sizes, has been acquired (Chapter 5). The importance of clouds for radiative, photochemical and dynamical processes is increasingly revealed in the atmospheric observations (see Chapters 4–6 and 9–13).

A second major achievement of modern exploration has been the improved vertical profiling at half-scale height resolution (~5 km) of temperature, dust, and water ice aerosol (McCleese et al., 2010; Chapters 4, 5, 10, and 11). Building on earlier work (Wilson, 2000), these have revealed the long-sought global signatures of thermal tidal wave structure in the interior atmosphere (Lee et al., 2009; Chapters 4, 5, 9, and 11). The non-uniformity of dust mixing in the lower atmosphere (Heavens et al., 2011, 2014; Chapters 4 and 10) was long suspected, but is now proven. The potent radiative drive of even thin ice clouds (Kleinböhl et al., 2013; Chapters 5, 6, 9, and 11) was also revealed.

The combination of higher spatial observing and of an extended record of observation has also provided clear evidence that Mars is changing today. Many sand dunes are observed to move (Bridges et al., 2012a,b), seasonal CO_2 slab ice subliming in the spring at high latitudes produces a variety of surface patterns (Hansen et al., 2010, 2013, 2015), and repeat observations have revealed recurring slope lineae (RSL), enigmatic albedo features a few meters wide which darken during the warm seasons, elongate downslope, and then fade away until the following Mars year, when the patterns repeat again (McEwen et al., 2014).

These databases are still being analyzed today and new observations continue to be acquired. In the next section, our current state of knowledge about the Mars atmosphere and climate is previewed, pointing to the more detailed discussions in the following chapters. This overview is divided into three connecting, but distinct, periods of Mars climate evolution: early Mars, with its more Earth-like climate; middle Mars, with its suggested ice ages driven by obliquity and orbital cycle variations; and modern Mars, still changing today.

2.5 MARS ATMOSPHERIC PHENOMENA: WHERE ARE WE NOW?

2.5.1 Early Mars

Billions of years ago, water did flow across its surface in great quantities, imprinting channels and other features on its ancient surface (Chapter 17). Groundwater levels rose and fell, altering the volcanic rock to produce aqueous minerals (e.g. carbonates, clays, sulfates). Exposed at the surface today, those minerals indicate a diversity of ancient surface environments, with different levels of acidity and processes operating at different

[1] Throughout the book, we use the abbreviations Ma (mega-annum) and Ga (giga-annum) to denote millions and billions of years of geological age (ago), respectively; and Myr and Gyr to denote time spans of millions and billions of years.

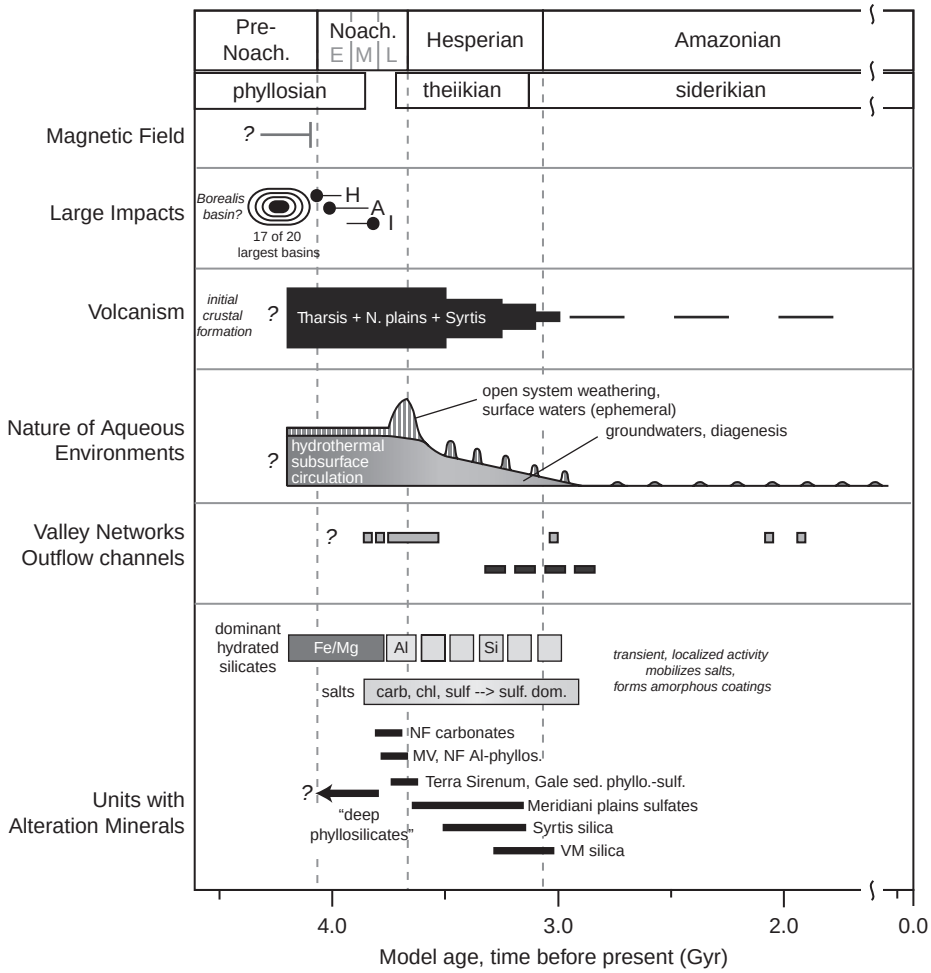

Figure 2.2. Mars through time. The chart shows major impact, volcanic, and fluvial events on Mars as dated by crater counting. The evidence for aqueous environments comes from both morphology (e.g. channels and valley networks) and composition, looking at the locations where surface composition reveals minerals whose formation requires the action of (liquid) water. These two ways of looking at Mars history can each be used to describe coherent epochs of Mars history. The traditional one uses the terms pre-Noachian (prior to 4.1 Ga), Noachian (4.1–3.7 Ga), Hesperian (3.7–3.1 Ga), and Amazonian (3.1 Ga to present). It is the early, apparently wetter, climate at the Noachian–Hesperian boundary that has long intrigued climatologists – and biologists – because of the possibly more Earth-like climate then. After Ehlmann et al. (2011).

temperatures. Ancient rocks dating from a time on Mars comparable to the time that life originated on Earth (~3.5 billion years) still survive on vast stretches of Mars, while they have been largely removed on the Earth through crustal subduction. For the atmosphere, the clues of that ancient past and subsequent evolution are contained in the rocks (see below) and in the trace gases of the atmosphere, including isotopes (e.g. Mahaffy et al., 2013).

The geochemical timeline shown in Figure 2.2 (Ehlmann et al., 2011) has been derived from multiple analyses based on data provided by the post-Viking wave of spacecraft exploration. It suggests an early period of high water activity, though in what form (groundwater, transient lakes and seas, precipitation – or all at different times) is highly debated. Nevertheless, there seems to have been a chemical evolution – perhaps episodic – from alteration of the ancient crust by more neutral pH water (e.g. producing clays) to later action by more acidic water (e.g. producing sulfates) (e.g. Murchie et al., 2009; Ehlmann and Edwards, 2014). The Curiosity Rover has been working its way toward a set of stratigraphic layers in the lower elevations of Mt. Sharp, the central peak of Gale Crater, that encompass this climate transition. Over the next few years, its analytic laboratories will tell us more about this geologically preserved record of change on early Mars. However, as high-spatial-resolution orbiter coverage of surface composition has expanded, with growing confidence in identification of various mineral types, there appear to have been periods when these different environments (e.g. neutral or high pH) either coexisted or repeated episodically, producing a more complex record. In any case, both orbiter and lander data are consistent with the alteration occurring in shallow seas or lakes and as a result of alteration by groundwater on early Mars. The debate about regional seas or an ocean (e.g. Di Achille and Hynek, 2010) and the role of precipitation continues (Chapter 17).

Ages of the surface material are derived from crater counting: the more heavily cratered a surface is, the older it is. Radiometric dating of Martian meteorites has been done on

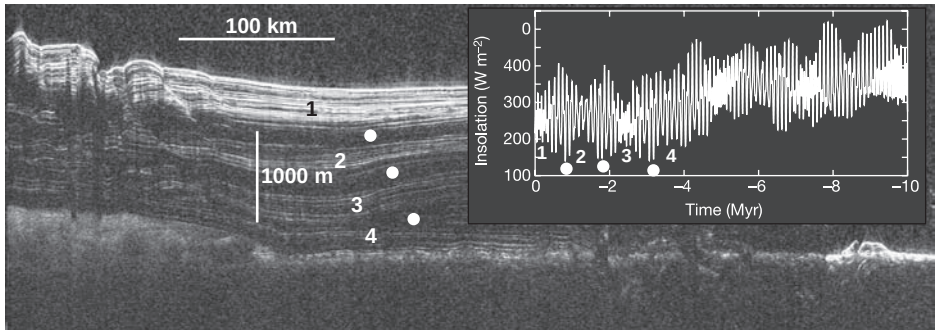

Figure 2.3. (Left) SHARAD radar reflections (Phillips et al., 2008) from depth through more than a kilometer of ice forming the north polar ice cap. Bright lines are radar reflections from layer interfaces, while dark areas have little radar return, presumably from cleaner ice. Note that the layers seem to come in "packets" of bright interfaces separated by darker bands. (Right) The packets are numbered and may correspond to periods of moderate polar irradiation due to obliquity variations (Laskar et al., 2004), when polar ice tends to sublime overall, leaving dustier (more reflective) layers. The darker areas (dots) correspond to periods of minimum polar irradiation, when relatively pure ice may condense overall.

Earth (most are geologically young), but the locations where the meteorites were blasted off the Martian surface are unknown, thus making it difficult to establish their geological context. An intriguing result from Curiosity analyzing drilled material in Gale Crater is that, while the rocks of the Gale Crater locale formed ~3.5 billion years ago (in agreement with crater counts), some of those rocks have been only recently exposed at the surface (~80 million years ago; Farley et al., 2013). This provides clues about the rates and timing of erosion and also points to places where organic material or other bio-signatures could be protected from ultraviolet and cosmic radiation for very long periods of time. In particular, there may have been more massive, probably episodic, erosion in relatively recent geologic times on Mars.

Both the meteoritic record and the *in situ* isotopic measurements made on Mars indicate that there has been massive atmospheric loss. Whether that is related to the early loss of a global magnetic field is still debated. If Mars once had a massive CO_2 atmosphere, which drove an Earth-like hydrologic cycle with precipitation and sustained liquid water on its surface, one path for its loss is the formation of carbonate at the Martian surface (Fanale et al., 1982; Kahn, 1985; Pollack et al., 1987). While carbonate has been detected, the volume of exposed carbonate (equivalent to ≤12 hPa of atmospheric CO_2; Edwards and Ehlmann, 2015) is much less than the hundreds of millibars often invoked in an attempt to simulate an early hydrosphere (Chapter 17).

If the Mars climate was much wetter early in its history, as the surface morphology and composition indicate, where has that water gone? As discussed above, there is evidence both for escape and for buried reservoirs of ice and hydrated materials in the crust (Chapters 15–17).

2.5.2 Middle Mars

The lure of a more Earth-like climate on ancient Mars, a time when life may have started on two planets in our Solar System, has sometimes eclipsed the fact that Mars may have undergone some dramatic climate changes in geologically more recent times; i.e. the middle and late Amazonian periods (Figure 2.2) have attractions of their own. The two polar caps are geologically young, but differ in many key respects, perhaps due to their different elevations. The north polar cap exposed during summer is a mile-thick slab of ice, with a semi-regular pattern of internal layering; it is also relatively young (≤10 million years, based on the flatness of the ground beneath it and the number of craters on its surface). The south polar cap appears much older (a few hundred million years), with its internal layers being much less regular (Phillips et al., 2008, and references therein). Furthermore, the south polar cap appears to contain enough buried CO_2 ice today that, if it were sublimed into the atmosphere, the resulting gas could double the present atmospheric mass (Phillips et al., 2011). At that point, much more of the surface could have pressures above the triple point of water, with more widespread transient liquid water (longer portions of a day and more days in the warm seasons). Such scenarios are now being investigated, with a goal of identifying what and where the physical evidence of such water activity would be.

The layering internal to the polar caps and exposed at their peripheries is due to the varying amounts of dust and ice, with dust being darker visually but more radar-reflective (bright). Whether the cameras and radars are viewing the same physical structures continues to be investigated – both see "packets" of layers suggesting deposition and erosion of layers of volatiles occurring on quasi-periodic timescales (Figure 2.3, Chapters 10, 11, and 16).

The prime source of the water that cycles over Mars each year today is the north polar ice cap. That ice cap is "permanent" in today's climate in the sense that a cap remains at the end of each water ice sublimation season. The amount of water that sublimes is dependent on the solar insolation absorbed by the polar cap and so is dependent on variations over thousands and millions of years of planetary obliquity and orbital eccentricity and phasing (Chapter 16). Figure 2.3 shows the radar-detected internal structure of the north polar cap that, together with the layers seen at the cap edge, suggests ice ages driven by the changes in polar insolation due to changes in the tilt of the Mars rotation axis (obliquity) and to changes in orbital eccentricity and its phasing (Chapters 10, 11, and 16).

Similar Milankovitch cycles are thought to drive ice ages on Earth. These astronomical cycles of insolation are more pronounced for Mars than for Earth. Compared to Earth, Mars

is a lumpy planet without oceans and the stabilizing influence of a large Moon; it is also closer to the gas giants of the outer Solar System (especially Jupiter) and thus more subject to their gravitational pull. In particular, while the axial tilt of Earth may vary by a degree or so, that of Mars varies by tens of degrees on timescales of a few hundred thousand to a few million years (Figure 2.3). Further, these variations for Mars are sufficiently chaotic that they cannot be deterministically calculated more than 20 million years into the past for the planetary parameters known today. However, it can be estimated statistically that, while Mars obliquity can range from nearly zero to above 60°, the "average" obliquity is ~40° (Laskar et al., 2004; Chapter 16).

One possible constraint on these ice ages would be characterizing the shallow ice distribution in mid-latitudes at depths of a few meters, greater than probed by the orbital high-energy spectrometers. Today this is being done by detecting new surface albedo changes using moderate-resolution cameras, with their more extensive coverage, and then confirming at higher resolution that the change has the signature of a new impact crater. Moderate-sized meteors (~1 m) can make it through the thin Mars atmosphere and the craters they produce excavate a few meters deep. Some of the over 500 new impact craters detected by MRO in the last 10 years (Byrne et al., 2009; Daubar et al., 2013) have white (icy) bottoms, which eventually go away as the exposed ice sublimes into the atmosphere (Dundas et al., 2014). These have moved the "ice boundary" closer to low latitudes, and the exact location of that boundary would have implications for the ice age scenarios (Chamberlain and Boynton, 2007).

2.5.3 Modern Mars: the Present Atmosphere

For transported aerosols and volatiles, the concept of cycles is a useful framework for understanding where things come from (sources), how they move elsewhere (transport), and where they end up (sinks). As discussed in *Mars* (Kieffer et al., 1992), Viking data enabled quantitative estimation of the principal components of these cycles for dust, water, and carbon dioxide. These cycles are all coupled in at least three ways (Chapters 4–13): (1) the transport circulation (dynamics, including interactions with the surface; Chapters 7–9); (2) the radiation fields that drive photochemistry (Chapter 13) and the circulation, responding to radiatively active gases and aerosols (Chapters 4–6); and (3) microphysics, which directly transforms the physical state of volatiles through sublimation and condensation, e.g. dust acting as ice cloud condensation nuclei, while condensing ice scavenges dust from the atmosphere (Chapters 10 and 11). While the basic outline of these cycles could be filled in using Viking data (as in *Mars*), many features remained uncertain, but fortunately much has been learned from data obtained by the latest wave of spacecraft exploration and its analysis and simulation.

The seasonal cycles of temperature, dust, ice, and water vapor have been observed for almost a full Mars decade and are discussed in detail in Chapters 4, 5, and 10–12. However, many questions remain. Are the annual cycles of water and carbon dioxide closed? For example, is the north polar cap gaining or losing water ice in the present climate? Is the thin carbon dioxide ice cover of the south polar cap disappearing or re-forming on timescales of a few decades (Thomas et al., 2014, 2016; Chapter 16)? Are the RSL truly the result of melted water ice forming brine flows (McEwen et al., 2014; Ojha et al., 2015)?

The dust cycle is particularly puzzling because of its interannual variability, with the largest storms occurring in some years, but not others. While regional dust events are likely to occur in particular seasonal windows, the processes by which some events grow to planetary scale in some years but not others remain a subject of intense research (Chapters 8–10). A recent hypothesis even implicates a contribution by the Sun–Mars motion around the Solar System's barycenter as a trigger to the largest events (Shirley, 2015; Chapters 8–10).

The thin CO_2 cover capping the south pole "permanent" cap is also a puzzle, as the pits (an arabesque "Swiss cheese" terrain) on the CO_2 cover expand with time (Malin et al., 2001) while other areas brighten, making the long-term effects uncertain (Thomas et al., 2014, 2016). Meanwhile the quantity of CO_2 snow contributing to the seasonal polar cap – as opposed to frost at the surface – has been estimated for the first time and could play a role, given that its emissivity differs from that of frost, to the uneven seasonal sublimation (Hayne et al., 2012, 2014).

Transport couples all these cycles. Winds raise the dust, which absorbs sunlight, heating the atmosphere, and changing the temperatures and winds. Dust is removed by scavenging due to formation of water ice crystals. The circulation redistributes carbon dioxide, whose seasonal sublimation and condensation are driven by the polar radiation balance (Chapters 6 and 12). Modeling atmospheric dynamics is discussed in detail in Chapters 8 and 9. The adequacy of these models can be viewed in the detailed discussions of the planetary boundary layer (Chapter 7), of the various cycles of dust, water, and carbon dioxide (Chapters 10–12), of atmospheric photochemistry (Chapter 13), of the upper atmosphere (Chapters 14 and 15), and of early climate (Chapter 17).

Radiation is the ultimate driver of the atmospheric processes (Chapter 6), while the radiative and energetic interactions between the atmosphere and space are discussed in Chapter 15. Microphysics are naturally discussed in many chapters, but particularly Chapters 5 and 10–12, as it is the microphysical processes that also link various components of the primary volatile and dust cycles.

In the book *Mars* (Kieffer et al., 1992), a common hope for the future was the acquisition of global, long-term datasets and improvements in atmospheric models. Much new data has been acquired (Chapter 3). Despite this bonanza, there are limitations. Coverage and vertical resolution near the surface are poor, in part because of dust opacity. While column abundances of water vapor (and carbon monoxide) have been retrieved, the vertical variation of water vapor is largely unobserved. And it would be useful to have another planetary-scale dust event during which our current orbiters observe the mechanics and environment of dust storm onset in detail; this, of course, depends on Mars. A major deficiency is the lack of wind observations. General limitations are the lack of synoptic and full diurnal coverage, and the lack of surface meteorological networks with simultaneous measurements over extended areas. Surface meteorological packages on Curiosity and a planned

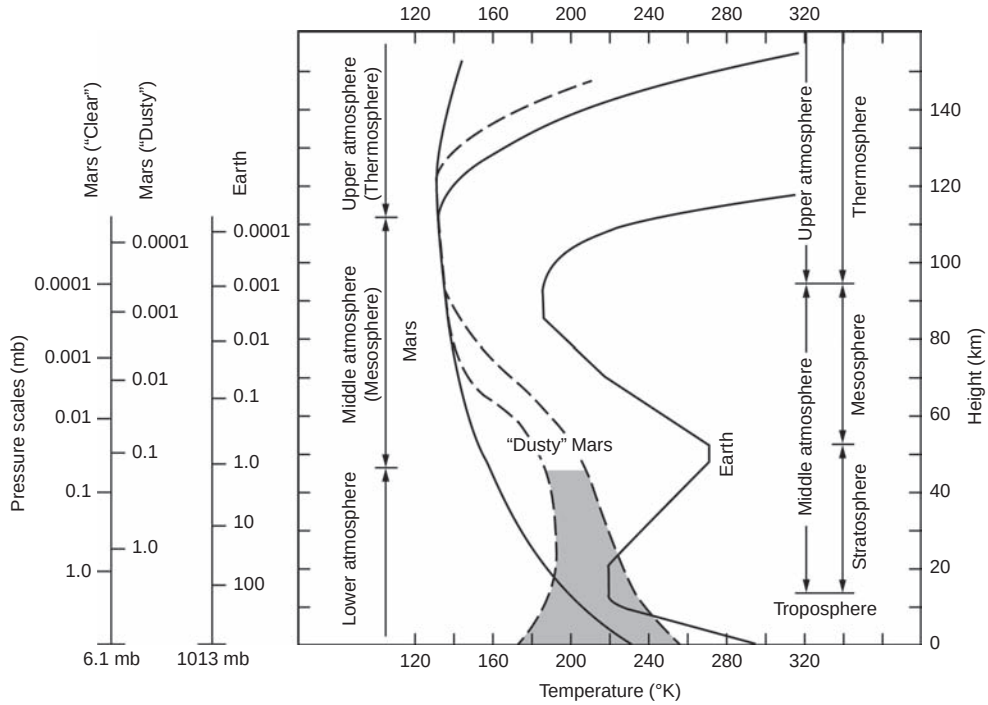

Figure 2.4. The U.S. standard atmosphere, published for the year in which the Viking Landers entered the Mars atmosphere, is shown (solid curve on the right) with the standard nomenclature for terrestrial meteorology. Temperatures derived from the Viking Lander 1 entry (Seiff and Kirk, 1977) serves here as a "standard reference atmosphere" for Mars, with similar nomenclature. Dashed curves with shading reflect the effects on temperature of aerosols during major dust events. Note the different hydrostatic pressure profiles on the left. Figure from Zurek (1992).

2020 Mars rover suffer from lack of vertical profiling above the platforms and from the inadvertent effects of the lander or rover supporting them. Some of these deficiencies may be addressed by a new orbiter, the ESA ExoMars Trace Gas Orbiter (TGO) launched in March 2016. After arrival at Mars in September and following a year of aerobraking, it will acquire new measurements from a ~400 km orbit drifting in local time.

Despite these limitations, as shown in the following chapters, the richness of the acquired data has added much to our understanding of the present cycles of dust, water, and carbon dioxide, and of the weather and climate of the planet.

As also hoped by the authors in *Mars*, atmospheric models have gone far beyond the 5°×7° latitude–longitude, six-level models of the Viking days (Pollack et al., 1976; Chapter 9). Ever greater computing power has enabled 50–100 levels in GCMs, extending model tops to 80 km or into the thermosphere (e.g. Forget et al., 1999; Richardson et al., 2007; Chapters 9 and 14). Annual simulations have been run at resolutions as fine as 1.5°×3° in latitude–longitude and mesoscale models have simulated regions at even higher resolution (Chapter 8). Interactive model runs in which dust is injected, transported around, and then removed from the atmosphere using physical parameterizations, including options for the radiative effects of the dust, are now possible. The effects of ice particle formation on dust and, through the ice aerosol radiative properties, on the general circulation, are now included in many models (Chapters 8–11).

The difficulty is that – as on Earth – the interaction between water and aerosols is complex and challenging, as the models try to bridge the gap between microphysical processes in the atmosphere and surface all the way to the global circulation. It was once thought (hoped?) that Mars would prove to be a simpler climate system than Earth, given the lack of latent heating by the condensation of significant amounts of water vapor. Measurements, however, have shown that clouds are as important for Mars as for Earth when simulating their climates (Chapters 5, 9, and 11). This is a significant change from the perspective expressed in *Mars*. Furthermore, attempts to understand the ancient climate of Mars (Chapter 17), when conditions may have been more Earth-like, may still require treatments of a full hydrological cycle (thick clouds with precipitation).

2.6 BASIC PARAMETERS AND NOMENCLATURE

2.6.1 Temperature

Figure 2.4 reproduces the "standard" temperature profile and nomenclature for Mars (left) and Earth (curve on right) from the book *Mars* (Kieffer et al., 1992). Although this "standard" Mars profile was based on the Viking entry profile (Seiff and Kirk, 1977), it is remarkably similar to the average of millions of temperature profiles retrieved by the MRO Mars Climate Sounder (Figure 4.2). Chapter 4 discusses in detail temperatures derived from multiple instruments and presents tables and graphs of "standard" profiles for Mars. The nomenclature still applies: The division between the upper and lower atmosphere – i.e. the mesopause or base of the thermosphere – occurs at altitudes ~100 km above the surface of both planets. The similarity of pressure near the mesopause on both planets is somewhat

remarkable given the different surface pressures: on Earth, 6.1 hPa occurs in the stratosphere at ~40 km altitude, while it is the surface pressure on Mars (Figure 2.4). On Mars, the lower gravity (resulting in a larger scale height) hydrostatically produces less change of pressure with height.

Above the mesopause, temperatures begin to increase due to the absorption of extreme ultraviolet radiation (Chapter 14). Below this level, the atmosphere on Mars can be divided into two regions, with the middle atmosphere (~50–100 km) marked by a more isothermal region (in reality with superposed waves; see Chapter 4). Near the surface, a planetary boundary layer exists, driven by convective and radiative transfer with the surface; its thickness and stability strongly vary throughout the diurnal cycle (Chapter 7).

The altitude separating the middle and lower regions varies significantly with atmospheric dust opacity, as well as season and geography. It is only during the planetary-scale dust events that Mars has something resembling the Earth's stratosphere, with solar heating of the airborne dust temporarily producing nearly isothermal zones or deep inversions comparable to the effect of ozone heating on Earth. Of course, individual temperature profiles do not vary smoothly with height as shown in Figure 2.4, but have pronounced wave structure, changing with time of day (Chapter 4; e.g. Figure 4.1). Such structures are a more pronounced category of variation on Mars than are their terrestrial counterparts (Chapters 4 and 9).

2.6.2 Clouds

Telescopic detection of distinct clouds was sufficiently rare that it was a noteworthy event. The major attributes recorded were the size, location, and color. The polar hazes were well known, obscuring the skies above the wintertime polar caps. Elsewhere, the two main categories of cloud were distinguished by color: white (presumed to be water-laden) or yellow (presumed to be composed of dust). As the low temperature of the atmosphere became better known, the water in the white clouds was assumed to be water ice (not droplets), and this was confirmed by the Mariner 9 Orbiter (Curran et al., 1973). The origin of the most recurrent of the white clouds (e.g. as in the historical Tharsis clouds or the Olympus "ring" cloud) became better understood once Mariner 9 revealed the topography: these were daily recurrences of orographically forced clouds, appearing prominently on the flanks of the massive Mars volcanoes. Chapter 5 provides a detailed description of cloud morphologies and occurrences.

2.6.3 Dust Storms and Mars Years

Originally, a dust storm was a yellow cloud that was observed to move. Telescopic observers recorded extensive dust storms (i.e. moving clouds that obscured large areas) in 1922 that lasted just four days, with a more prominent and longer-lived storm in 1956. The 1956 event was well documented by many astronomers thanks to an international coordinating effort. It was regarded as truly exceptional (Slipher, 1962) until 1971 when the International Planetary Patrol alerted NASA that a global dust storm awaited its Mariner 9 spacecraft. In recent times, many scientists working with spacecraft observations have followed Clancy et al. (2000) by counting Mars years referenced to designating the Mars year in which this vast storm occurred as Mars Year 1 (MY 1) (1 MY = 1.88 years). Currently, it is MY 33, which began with the Martian northern spring equinox (L_s = 0°) on June 18, 2015.

The reference to the largest-scale events as global dust storms (GDS) began with the descriptions and discussions of the possible origin of the 1971 storm that was still raging when Mariner 9 entered Mars orbit (Gierasch, 1974). That truly global event extended from pole to pole. Of two very large events observed by the Viking Orbiters, the first was more hemispheric, while the second affected both hemispheres; neither was as global as the 1971 GDS, and nothing of that scale occurred in the second Viking year. Thus, the GDS nomenclature became great dust storms, associated with obscurations that encircled Mars or covered regions comparable to a planetary radius or more in size, i.e. planetary scale (Zurek, 1982). Furthermore, these new data combined with historic Earth-based observations suggested that the largest dust storms tended to occur in southern spring and summer, the so-called (large or great) "dust storm season". It is important to remember that smaller dust storms occur every Mars year and in every season, although their frequency and place of occurrence vary throughout the year (Chapter 10).

The dust hazes are far more extensive than the dust raising regions themselves, and some researchers have restricted the use of "dust storm" to indicate only those areas where dust is actively being raised into the atmosphere. Both Earth-based telescopic and spacecraft imagers have shown that the planetary-scale events typically have multiple centers of dust raising; this may even be necessary to produce a planetary-scale haze, even though a single local dust storm may be a trigger. To keep up with the added insight provided by daily global coverage that recent orbiters have produced for nearly 17 years, the ensemble of dust raising zones and associated dust hazes obscuring a major fraction of the planet is often referred to as a dust "event". Chapter 10 provides a modern description of the dust cycle and these episodic events.

Table 2.1 shows basic properties of Mars in terms of size, mass, rotation, and orbital parameters, contrasting these with Earth. Clearly, Mars and Earth share some fundamental properties. While smaller than the Earth, the surface area of Mars is nearly the same as the land area of the Earth. The fast rotation of the planets means that much of the meteorological theory developed for Earth should be applicable to Mars, and so we have confidence that the meteorological models developed for Earth can be adapted to Mars.

Table 2.2 (also Chapter 4) shows the basic composition of the atmosphere of Mars, which has been updated using the recent measurements by the analytical laboratory on the Curiosity Rover (Mahaffy et al., 2013). Although largely carbon dioxide, the atmosphere contains several trace gases whose isotopes are useful in understanding the age and exposure of the surface (Farley et al., 2013), the amount of atmosphere loss that may have occurred, and as tracers of transport (e.g. water vapor, carbon monoxide, and argon). Searches for other trace gases (e.g. methane) continue, as they could be signatures of biological and/or geochemical processes.

Table 2.2. *Atmospheric composition and other data.*

	Mars	Earth	Ratio
Composition (vol.%)[a]			
Carbon dioxide CO_2	0.960	0.00036	
Argon Ar	0.0193	0.00934	
Nitrogen N_2	0.0189	0.781	
Oxygen O_2	0.00145	0.209	
Mean molecular weight, m_w (g mol^{-1})	43.6	29.0	
Gas constant, $R = R^*/m_w$ (J K^{-1} kg^{-1})	191	287	
Specific heat, c_p (at 200 K) (J K^{-1} kg^{-1})	735	1000	
$\kappa = R/c_p$	0.259	0.287	
Ratio of specific heats, $\gamma = c_p/c_v$	1.2	1.4	
Surface pressure[b] (at mean radius) (hPa)	6.3	1013	0.62%
Column mass[b] (mean) (kg m^{-2})	170	1030	1.65%
Column water (pr cm water equivalent)[b]	<0.0008	≤8	~0.01%
Planetary equilibrium temperature, T_e (K)	210	256	0.82
Adiabatic temp. lapse rate, $-g/c_p$ (K km^{-1})	−5.0	−9.8	0.47
Radiative time constant (days)	~2	≥20	~10%

[a] Mahaffy et al. (2013).
[b] These quantities are highly variable on Mars, much more than the ~10% variation on Earth.

Table 2.3. *Dynamical parameters for Mars and Earth.*

Parameter	Mars	Earth	Units
Scale height (lower atmos.), T_eR/g	10.8	7.5	km
Equatorial rotation speed, $a\Omega$	241	465	m s^{-1}
External gravity wave speed, $(gH)^{1/2}$	200	271	m s^{-1}
Lamb's parameter, $4(a\Omega)^2/gH$	5.8	11.8	—
Speed of sound, $(\gamma gH)^{1/2}$	219	321	m s^{-1}
Typical lapse rate (just above boundary layer)	−2.5	−6.5	K km^{-1}
Brunt–Väisälä frequency, N	0.67×10^{-2}	1.12×10^{-2}	s^{-1}
Internal gravity wave speed, NH	72	84	m s^{-1}
Rossby radius of deformation, NH/Ω	1022	1154	km

In Table 2.3 some basic meteorological scaling parameters are also shown. Again, it is the similarities in some, but not all, that makes Mars a high-priority object for comparative study.

2.7 SUMMARY

As noted in the Introduction (Chapter 1), the existence of other planets in our Solar System (and now known to be around other stars, as well) provides natural laboratories that can test our theories and our tools for understanding planetary climates, including our own. Mars plays a special role in comparison with Earth, given its many fundamental similarities – rapid rotation, seasons, and sunlight largely absorbed at its surface – and its key differences – its greater distance from the Sun, a mostly CO_2 atmosphere which seasonally condenses and sublimes, little if any surface water today, and no global magnetic field at present. The similarities mean our terrestrial models should be applicable to Mars, while the differences can truly test our hypotheses of atmospheric behavior, when we have the needed data. This is certainly true for modern Earth and Mars, but an equally intriguing comparison is that of modern Earth and ancient Mars – the more Earth-like Mars with water coursing across its surface, shallow lakes and possibly seas, a thicker atmosphere shielded by a global magnetic field. And, finally, that ancient Mars with its rock record still preserved today may tell us about early Earth and early planetary development.

The compelling human interests that today drive exploration in the 21st century are much the same as those that engaged the public early in the 20th, when Lowell and other astronomers were trying to make sense of what they saw. Those interests are expressed today as follows:

- *Life*. Are we alone in this Universe? Did life develop on Mars, perhaps in a more Earth-like early environment? If so, is there evidence of that life preserved on the planet today? Is there life even today on or near its surface? Life on Earth has dramatically affected our atmosphere and climate. What happened on Mars?
- *Climate*. There is evidence that the climate of Mars was different in the past – why? How much is the climate changing today? Can Mars give us clues as to *how* planetary climates change, providing insight into the past and future climates of our own planet?
- *Destination*. Of all the planets, it seemed then, as well as now, that Mars would be most hospitable to explorers from Earth.

These remain compelling themes of Mars exploration.

Today's observations of the present planet are the best means of establishing what its present climate is and how it may have changed. As in the past, atmospheric circulation/climate models remain the best integrators of climate processes as we understand them. They permit us to explore the uncertainties and the possible roles of new physical processes needed to truly understand the Martian climate and its evolution. The data tell us whether the models have the right processes working in the proper way. The current data already tell us that we still have much to learn, even given the impressive returns from our latest (third) wave of space exploration. We still lack key information needed to

describe the current Martian atmospheric state and circulation; such data are also needed for validation and improvement of atmospheric models. Some high-priority goals are observations of winds and of detailed boundary layer processes and microphysical processes generally. This is true even after a half-century of space observation, analyses, and model development.

All the current space missions are in extended operations; several (Opportunity, MEX, ODY, MRO) are still returning highly valuable data a decade or more after their launch, while Curiosity, MOM, and MAVEN continue to explore, building on their prime missions. This is a testament to the excellent technical capabilities of the spacecraft and payloads and to the dedicated efforts of the hundreds of women and men who built, launched, and then operated them – and those who continue do so even now.

If we are to have confidence in our understanding of the present and past atmosphere of Mars, we need the data that these aging but capable assets continue to provide, and we also need to fill the many key data gaps with new missions that have the technical capabilities to make the necessary advances in observing (Chapter 18). And we need to continue to improve our models, which continue to be our best means for integrating diverse datasets and physical intuition and for ultimately understanding the impressive climate change that has occurred on Mars.

For now, however, the reader is invited into the further discussions of our present understanding of the atmosphere and climate of Mars, remembering that such understanding is rooted in observational coverage in time and space that is unprecedented – despite its limitations – for any other planet except, of course, our own Earth.

ACKNOWLEDGMENTS

The writing and research of this chapter was carried out at the Jet Propulsion Laboratory, California Institute of Technology, under a contract with the National Aeronautics and Space Administration.

REFERENCES

Acuna, M. H., J. E. P. Connerney, N. F. Ness, et al. (1999), Global distribution of crustal magnetization discovered by the Mars Global Surveyor MAG/ER experiment. *Science* 284: 790–793, doi:10.1126/science.284.5415.790.

Anderson, E. M. and C. B. Leovy (1978), Mariner 9 television limb observations of dust and ice hazes on Mars. *J. Atmos. Sci*. 35: 723–734.

Boynton, W. V., W. C. Feldman, S. W. Squyres, et al. (2002), Distribution of hydrogen in the near surface of Mars: evidence for subsurface ice deposits. *Science* 297: 81–85, doi:10.1126/science.1073722.

Bridges, N., F. Ayoub, J.-P. Avouac, et al. (2012a), Earth-like sand fluxes on Mars. *Nature* 485: 339–342, doi:10.1038/nature11022.

Bridges, N., M. C. Bourke, P. E. Geissler, et al. (2012b), Planet-wide sand motion on Mars. *Geology* 40: 31–34, doi:10.1130/G23273.1.

Byrne, S., C. M. Dundas, M. R. Kennedy, et al. (2009), Distribution of mid-latitude ground ice on Mars from new impact craters. *Science* 325: 1674–1676, doi:10.1126/science.1175307.

Cassini (1666), *J. Savants* 2: 316.

Chamberlain, M. A., and W. V. Boynton (2007), Response of Martian ground ice to orbit-induced climate change. *J. Geophysical Res.–Planets* 112, doi:10.1029/2006JE002801.

Chapman, S., and R. S Lindzen (1970), *Atmospheric Tides* (New York: Gordon and Breach).

Clancy, R. T., B. J. Sandor, M. J. Wolff, et al. (2000), An intercomparison of ground-based millimeter, MGS TES, and Viking atmospheric temperature measurements: seasonal and interannual variability of temperatures and dust loading in the global Mars atmosphere. *J. Geophys. Res*. 105: 9553–9571.

Coblentz, W. W., and C. O. Lampland (1927), Further radiometric measurements and temperature estimates of the planet Mars. *Sci. Paper Natl. Bur. Stds*. 22: 237–276.

Conrath, B. J. (1976), Influence of planetary-scale topography on the diurnal thermal tide during the 1971 Martian dust storm. *J. Atmos. Sci*. 33: 2430–2439.

Curran, R. J., B. J. Conrath, R. A. Hanel, V. G. Kunde, and J. C. Pearl (1973), Mars: Mariner 9 spectroscopic evidence for H_2O ice clouds. *Science* 182: 381–383.

Daubar, I. J., A. S. McEwen, S. Byrne, M. R. Kennedy, and B. Ivanov (2013), The current Martian cratering rate. *Icarus* 225: 506–516, doi:10.1016/j.icarus.2013.4.9.

De Vaucouleurs, G. (1954), *Physics of the Planet Mars* (London: Faber and Faber).

Di Achille, G., and B. M. Hynek (2010), Ancient ocean on Mars supported by global distribution of deltas and valleys. *Nature Geoscience* 3: 459–463.

Dundas, C. M., S. Byrne, A. S. McEwen, et al. (2014), HiRISE observations of new impact craters exposing Martian ground ice. *J. Geophys. Res.* 119, doi:10.1002/2013JE004482.

Edwards, C. S., and B. L. Ehlmann (2015), Carbon sequestration on Mars. *Geology* 43, doi:10.1130/G36983.1.

Ehlmann, B. L., and C. S. Edwards (2014), Mineralogy of the Martian surface. *Annual Review of Earth and Planetary Sciences* 42: 291–315, doi:10.1146/annurev-earth-060313-055024.

Ehlmann, B. L., J. F. Mustard, S. L. Murchie, et al. (2011), Subsurface water and clay mineral formation during the early history of Mars. *Nature* 479: 53–60, doi:10.1038/nature10582.

Fanale, F. P., J. R. Salvail, W. B. Banerdt, and R. S. Saunders (1982), Mars: the regolith–atmosphere–cap system and climate change. *Icarus* 50: 381–407.

Farley, K. A., C. Malespin, P. Mahaffy, et al. (2013), In situ radiometric and exposure age dating of the Martian surface. *Science* 343, doi:10.1126/science.1247166.

Farmer, C. B., D. W. Davies, A. L. Holland, D. D. Laporte, and P. E. Doms (1977), Mars: water vapor observations from the Viking Orbiters. *J. Geophys. Res.* 82: 4225–4248.

Feldman, W. C., W. V. Boynton, R. L. Tokar, et al. (2002), Global distribution of neutrons from Mars: results from Mars Odyssey. *Science* 297: 75–78, doi:10.1126/science.1073541.

Fergason, R. L., P. R. Christensen, and H. H. Kieffer (2006), High-resolution thermal inertia derived from the Thermal Emission Imaging System (THEMIS): thermal model and applications. *J. Geophys. Res.* 111, E12004, doi:10.1029/2006JE002735.

Forget, F., F. Hourdin, R. Fournier, et al. (1999), Improved general circulation models of the Martian atmosphere from the surface to above 80 km. *J. Geophys. Res.* 104: 24155–24176.

Gierasch, P. J. (1974), Martian dust storms. *Rev. Geophys. Space Phys*. 12: 730–734.

Gierasch, P. J., and R. M. Goody (1967), An approximate calculation of radiative heating and radiative equilibrium in the Martian atmosphere. *Planet. Space Sci.* 15: 1465–1477.

Gierasch, P. J., and R. M. Goody (1968), A study of the thermal and dynamical structure of the Martian lower atmosphere. *Planet. Space Sci.* 16: 615–646.

Gierasch, P. J., and R. M. Goody (1972), The effect of dust on the temperature of the Mars atmosphere. *J. Atmos. Sci*. 29: 400–402.

Goody, R. M., and M. J. S. Belton (1967), Radiative relaxation times for Mars: a discussion of Martian atmospheric dynamics. *Planet. Space Sci*. 15: 247–256.

Haberle R. M., C. B. Leovy and J. B. Pollack (1982), Some effects of global dust storms on the atmospheric circulation of Mars. *Icarus* 50: 322–367, doi:10.1016/0019-1035(82)90129-4.

Hanel, R. A., B. J. Conrath, W. A. Hovis, et al. (1972), Infrared spectroscopy experiment on the Mariner 9 mission: preliminary results. *Science* 175: 305–308.

Hansen, C. J., N. Thomas, G. Portyankina, et al. (2010), HiRISE observations of gas sublimation-driven activity in Mars southern polar regions: I. Erosion of the surface. *Icarus* 205: 283–295.

Hansen, C. J., S. Byrne, G. Portyankina, et al. (2013), Observations of the northern seasonal polar cap on Mars: I. Spring sublimation activity and processes. *Icarus* 225: 881–897.

Hansen, C. J., S. Diniega, N. Bridges, et al. (2015), Agents of change on Mars' northern dunes: CO_2 ice and wind. *Icarus*, 251: 264–274.

Hartmann, W. K., and O. Raper (1974), *The New Mars: The Discoveries of Mariner 9*, NASA SP-337 (Library of Congress Catalog Card #74-600084).

Hayne, P. O., D. A. Paige, J. T. Schofield, et al. (2012), Carbon dioxide snow clouds on Mars: south polar winter observations by the Mars Climate Sounder. *J. Geophys. Res*. 117, E08014, 10.1029/2011JE004040.

Hayne, P. O., D. A. Paige, N. G. Heavens, et al. (2014), The role of snowfall in forming the seasonal ice caps of Mars: models and constraints from the Mars Climate Sounder. *Icarus* 231: 122–130.

Heavens, N. G., M. I. Richardson, A. Kleinböhl, et al. (2011), The vertical distribution of dust in the Martian atmosphere during northern spring and summer: observations by the Mars Climate Sounder and analysis of zonal average vertical dust profiles. *J. Geophys. Res*., 116, E4, E04003, doi:10.1029/2010JE003691.

Heavens, N. G., M. S. Johnson, W. A. Abdou, et al. (2014), Seasonal and diurnal variability of detached dust layers in the Mars atmosphere. *J. Geophys. Res. Planets* 119: 1748–1774, doi:10.1002/2014JE004619.

Herschel, W. (1784), On the remarkable appearances of the polar regions of the planet Mars, the inclination of its axis, the position of its poles, and its spheroidical figure; with a few hints relating to its real diameter and atmosphere. *Phil. Trans*. 24: 233–273.

Hess, S. (1950), Some aspects of the meteorology of Mars. *J. Meteorol*. 7: 1–13.

Hess, S. L., R. M. Henry, C. B. Leovy, et al. (1977), Meteorological results from the surface of Mars: Viking 1 and 2. *J. Geophys. Res.* 82, 4559–4574.

Kahn, R. (1985), The evolution of CO_2 on Mars. *Icarus* 62: 175–190.

Kaplan, L. D., G. Munch, and H. Spinrad (1964), An analysis of the spectrum of Mars. *Astrophys. J*. 139: 1–15.

Kieffer, H., B. M. Jakosky, C. W. Snyder, and M. S. Mathews (Eds) (1992), *Mars* (Tucson, AZ: University of Arizona Press).

Kleinböhl, A., R. J. Wilson, D. Kass, J. T. Schofield, and D. J. McCleese (2013), The semidiurnal tide in the middle atmosphere of Mars, *Geophys. Res. Lett.* 40: 1952–1959, doi:10.1002/grl.50497.

Kuiper, G. P. (1952), *The Atmospheres of the Earth and Planets*, rev. ed. (Chicago: University of Chicago Press), 358–361.

Laskar, J., A. C. M. Correia, M. Gastineau, et al. (2004), Long term evolution and chaotic diffusion of the insolation quantities of Mars. *Icarus* 170: 343–364.

Lee, C., W. G. Lawson, M. I. Richardson, et al. (2009), Thermal tides in the Martian middle atmosphere as seen by the Mars Climate Sounder. *J. Geophys. Res*. 114, E03005, doi:10.1029/2008JE003285.

Leighton, R. B., and B. C. Murray (1966), Behavior of carbon dioxide and other volatiles on Mars. *Science* 153: 136–144.

Leovy, C. B. (1966), Note on thermal properties of Mars. *Icarus* 5: 1–6.

Leovy, C. B., and Y. Mintz (1969), Numerical simulation of the atmospheric circulation and climate of Mars. *J. Atmos. Sci*. 26: 1167–1190.

Lindzen, R. S. (1970), The application and applicability of terrestrial atmospheric tidal theory to Venus and Mars. *J. Atmos. Sci*., 27: 536–549.

Lowell, P. (1895), *Mars* (London: Longmans and Green).

Lowell, P. (1896), *Mars* (Boston: Houghton Mifflin).

Lowell, P. (1906), *Mars and Its Canals* (New York: Macmillan).

Lowell, P. (1908), *Mars as the Abode of Life* (New York: Macmillan).

Mahaffy, P. R., C. R. Webster, S. K. Atreya, et al. (2013), Abundance and isotopic composition of gases in the Martian atmosphere from the Curiosity Rover. *Science* 341: 263–266, doi:10.1126/science.1237966.

Malin, M. C., M. A. Caplinger, and S. D. Davis (2001), Observational evidence for an active surface reservoir of solid carbon dioxide on Mars. *Science* 294: 2146–2148, doi:10.1126/science.1066416.

Martin, L. J., P. B. James, A. Dollfus, K. Iwasaki, and J. Beish (1992), Comparative aspects of the climate of Mars: telescopic observations: visual, photographic, polarimetric. In *Mars*, ed. H. Kieffer et al. (Univ. Arizona Press, Tucson), 34–70.

McCleese, D. G., N. G. Heavens, J. T. Schofield, et al. (2010), The structure and dynamics of the Martian lower and middle atmosphere as observed by the Mars Climate Sounder: 1. Seasonal variations in zonal mean temperature, dust and water ice aerosols. *J. Geophys. Res.* 115, E12016, doi:10.1029/2010JE003677.

McEwen, A. S., C. M. Dundas, S. S. Mattson, et al. (2014), Recurring slope lineae in equatorial regions of Mars. *Nature Geoscience* 7: 53–58.

Mellon, M. T., R. E. Arvidson, H. G. Sizemore, et al. (2009), Ground ice at the Phoenix landing site: stability state and origin. *J. Geophys. Res*. 114, E00E07, doi:10.1029/2009JE003417.

Mintz, Y. (1961), The general circulation of planetary atmospheres. *The Atmospheres of Mars and Venus*, ed. Kellogg and C. Sagan, NAS-NRC Publ. 944: 107–146.

Mitrofanov, I., D. Anfimov, A. Lozyrev, et al. (2002), Maps of subsurface hydrogen from the high energy neutron detector, Mars Odyssey. *Science* 297: 78–81, doi:10.1126/science.1073616.

Murchie, S. L., J. Mustard, B. L. Ehlmann, et al. (2009), A synthesis of Martian aqueous mineralogy after 1 Mars year of observations from the Mars Reconnaissance Orbiter. *J. Geophys. Res*. 114, doi:10.1029/2009JE003342.

Ojha, L., M. B. Wilhelm, S. L. Murchie, et al. (2015), Spectral evidence for hydrated salts in recurring slope lineae on Mars. *Nature Geoscience* 8: 829–832, doi:10:1038/ngeo2546.

Owen, T. (1992) The composition and early history of the atmosphere of Mars. In *Mars*, ed. H. Kieffer et al. (Univ. Arizona Press, Tucson), 818–834.

Phillips, R. J., M. T. Zuber, S. E. Smrekar, et al. (2008), Mars north polar deposits: stratigraphy, age, and geodynamical response. *Science* 320: 1182–1185, doi:10.1126/science.1157546.

Phillips, R. J., B. J. Davis, K. L. Tanaka, et al. (2011), Massive CO_2 ice deposits sequestered in the south polar layered deposits of Mars. *Science* 332: 838–841, doi:10.1126/science.1203091.

Pollack, J. B., C. B. Leovy, Y. H. Mintz, and W. Van Camp (1976), Winds on Mars during the Viking season: predictions based on a general circulation model with topography. *Geophysical Research Letters* 3, doi:10.1029/GL003i008p00479.

Pollack, J. B., J. F. Kasting, S. M. Richardson, and K. Poliakoff (1987), The case for a wet, warm climate on early Mars. *Icarus* 71: 203–224.

Richardson, M. I., A. D. Toigo, and C. E. Newman (2007), PlanetWRF: a general purpose, local to global numerical model for planetary atmospheric and climate dynamics. *J. Geophys. Res.* 112, E09001, doi:10.1029/2006JE002825.

Sagan, C. A., and J. B. Pollack (1969), Windblown dust on Mars. *Nature* 223: 791–794.

Seiff, A., and D. B. Kirk (1977), Structure of the atmosphere of Mars in summer at mid-latitudes. *J. Geophys. Res*. 82: 4364–4378.

Shirley, J. H. (2015), Solar system dynamics and global-scale dust storms on Mars. *Icarus* 252: 128–144, 10.1016/j.icarus.2014.09.038.

Slipher, E. C. (1962), *The Photographic Story of Mars* (Flagstaff: Northland Press).

Smith, D. E., M. T. Zuber, S. C. Solomon, et al. (1999), The global topography of Mars and implications for surface evolution. *Science* 284: 1495–1503.

Smith, D. E., M. T. Zuber, H. V. Frey, et al. (2001), Mars Orbiter Laser Altimeter: experiment summary after the first year of global mapping of Mars. *J. Geophys. Res.: Planets* 106: 23689–23722.

Smith, P. H., L. K. Tamppari, R. E. Arvidson, et al. (2009), H_2O at the Phoenix landing site. *Science* 325: 58–61, doi:10.1126/science.1172339.

Spinrad, H., G., Munch, and L. D. Kaplan (1963), The detection of water vapor on Mars. *Astrophys. J*. 137: 1319–1321.

Spinrad, H., R. A. Schorn, R. Moore, L. P. Giver, and H. J. Smith (1966), High dispersion spectroscopic observations of Mars. I. The CO_2 content and surface pressure. *Astrophys. J*. 146: 331–338.

Stewart, A. I., C. A. Barth, C. W. Hord, and A. L. Lane (1972), Mariner 9 ultraviolet spectrometer experiment: structure of Mars upper atmosphere. *Icarus* 17: 469–474.

Tamppari, L., R. W. Zurek, and D. A. Paige (2000), Viking era water-ice clouds. *J. Geophys. Res.* 105: 4087–4107.

Thomas, P. C., W. Calvin, R. Haberle, et al. (2014), Mass balance of Mars' south polar residual cap from spacecraft imaging. In *Eighth International Conference on Mars*, LPI Contribution 1791: 1085.

Thomas, P. C., W. Calvin, B. Cantor, et al. (2016), Mass balance of Mars' residual south polar cap from CTX images and other data, *Icarus*, in press.

Tolson, R. H., G. M. Keating, R. W. Zurek, et al. (2007), Application of accelerometer data to atmospheric modeling during Mars aerobraking operations. *J. Spacecraft and Rockets* 44(6): (1172–1179).

Von Braun, W., and W. Ley (1956), *The Exploration of Mars* (New York: Viking Press).

Wallace, A. R. (1907), *Is Mars Habitable?* (London: Macmillan).

Wilson, R. J. (2000), Evidence for diurnal period Kelvin waves in the Martian atmosphere from Mars Global Surveyor TES data. *Geophys. Res. Lett*. 27(23): 3889–3892, doi:10.1029/2000GL012028.

Zurek, R. W. (1976), Diurnal tide in the Martian atmosphere. *J. Atmos. Sci*. 33: 321–337.

Zurek, R. W. (1980), Surface pressure response to elevated tidal heating sources: comparison of Earth and Mars. *J. Atmos. Sci*. 37: 1132–1136.

Zurek, R. W. (1982), Martian Dust Storms, An Update. *Icarus* 50: 288–310.

Zurek, R. W. (1992), Comparative aspects of the climate of Mars: an introduction to the current atmosphere. *Mars*, ed. H. Kieffer et al. (University of Arizona Press), Tucson, 799–817.

Zurek, R. W., and C. B. Leovy (1981), Thermal tides in the dusty Martian atmosphere: a verification of theory. *Science* 213 (4506): 437–439, doi:10.1126/science.213.4506.437.